ELSEVIER

Thermochimica Acta 335 (1999) 121–126

thermochimica acta

www.elsevier.com/locate/tca

The decomposition kinetics of nanocrystalline calcite

Linghai Yue, Miao shui, Zhude Xu*

Department of Chemistry, Zhejiang University, Hangzhou 310027, China

Received 16 February 1999; accepted 22 June 1999

Abstract

The decomposition kinetics of nanocrystalline calcite is investigated using the master plot method and Coats and Redfern's equation. It is shown that the nanocrystalline calcite as well as the reference calcite dissociates according to the contracting volume mechanism R_3. Comprehensive techniques have been used to determine the kinetic parameters. A considerable diminution of the activation energy E_a up to 70–80 kJ mol^{-1} is observed in the case of nanocrystalline calcite. In addition, the kinetic compensation law has also been used to correlate the pre-exponential factor A with the activation energy E_a. © 1999 Elsevier Science B.V. All rights reserved.

Keywords: Nanocrystalline calcite; Decomposition kinetics

1. Introduction

Calcium carbonate is one of the most widely used fillers in many industrial applications such as plastics, rubber, paper making and medicine. Recently it is found that the nano scale calcium carbonate has much more advantages than the commonly used normal size calcium carbonate and its novel characteristic has attracted wide research interests.

Extensive work has been carried out on the non-isothermal decomposition kinetics of solid system. Multiple techniques were reported in literatures for determining the reaction mechanism and deducing kinetic parameters [1–7]. Contrary to the homogeneous reaction, the mechanism and kinetics of solid decomposition will vary with many factors such as the change of reaction condition, crystal form and particle size. It is mainly owing to the influence of heat transfer and mass transfer on the phase boundaries. Since that, although the dissociation of calcium carbonate has been widely studied, its mechanism and kinetic parameters reported in the literatures are not well consistent [4,6,8]. Besides, to the nano scale particles, the kinetic behavior of decomposition is particularly rarely noticed. Criado and Ortega [9] has observed that smaller particle would result in the diminution of the activation energy, but their experiment was confined to particles of micro scale. As is known to all, constitutive particle size of nanomaterial is ranging between molecular cluster and bulk substance. It may result in many special characteristics. In this paper, the thermal decomposition of nanocrystalline calcite is studied to see the effect of particle size on the decomposition parameters and mechanism.

*Corresponding author. Tel.: +86-571-795-1352; fax: +86-571-795-1895.

PII: S0040-6031(99)00174-4

2. Decomposition kinetics

The commonly used equation in the non-isothermal decomposition kinetics is presented below

$$\frac{d\alpha}{dT} = kf(\alpha), \tag{1}$$

in which the kinetic function $f(\alpha)$ is determined by reaction mechanism and speed controlling step. It has an another form as

$$g(\alpha) = \int_0^{\alpha} \frac{d\alpha}{f(\alpha)}. \tag{2}$$

Possible $f(\alpha)$ and expressions are listed in Table 1.

Since the mechanism determination and the kinetic parameter calculation are mutually dependent, non-mechanism equation is firstly introduced to estimate the activation energy as a prerequisite for determining the reaction mechanism. After the reaction mechanism is deduced, mechanism equations are then used to further confirm the kinetic parameters obtained previously.

Freeman–Carroll [10] equation and Kissinger [11] equation are commonly used non-mechanism equations. However, There is evidence that the former may yield diffusive data points. So, Kissinger equation,

$$\ln(A) = \ln\left(\frac{E_a}{R}\right) - \ln\left(\frac{T_p^2}{\beta}\right) + \frac{E_a}{RT_p}, \tag{3}$$

is applied to estimate the activation energy where T_p represents the peak temperature of DTA curve, β is the heating rate. Although some authors suggested that T_m, peak temperature of DTG curve, rather than Tp should be used in the above formula [6,7], T_p is still preferred when the reaction proceeds over narrow temperature range (between 0.9 T_m and 1.1 T_m). In this case, T_p is very close to T_m and easy to accurately determined.

In the mechanism determining process, methods proposed by Berggern and Satava [12] (plot $\log(g(a))$ against $1/T$), and by Coats and Redfern [13] (plot $\log(g(a)/T^2)$ against $1/T$) are not sensitive enough to distinguish some mechanisms. Master plot method less influenced by experimental conditions is used

Table 1
Classification of kinetic models for reaction mechanism

Kinetic classification	$g(a) = \int d\alpha/f(\alpha)$	$f(\alpha)=(1/k)(d\alpha/dt)$
(1) Acceleratory $\alpha-t$ curves		
Powerlaw (P_1)	$\alpha^{1/n}$	$n\cdot\alpha^{(n-1)/n}$
Exponential law (E_1)	$\ln(\alpha)$	α
(2) Sigmoidal $\alpha-t$ curves		
Avrami–Erofeev (A_2)	$[-\ln(1-\alpha)]^{1/2}$	$2(1-\alpha)[-\ln(1-\alpha)]^{1/2}$
Avrami–Erofeev (A_3)	$[-\ln(1-\alpha)]^{1/3}$	$3(1-\alpha)[-\ln(1-\alpha)]^{2/3}$
Avrami–Erofeev (A_4)	$[-\ln(1-\alpha)]^{1/4}$	$4(1-\alpha)[-\ln(1-\alpha)]^{3/4}$
Prout–Tompkins (B_1)	$\ln[\alpha(1-\alpha)]+C$	$\alpha\cdot(1-\alpha)$
(3) Deceleratory $\alpha-t$ curves		
(3.1) Based on geometrical models		
Contracting area (R_2)	$1-(1-\alpha)^{1/2}$	$2(1-\alpha)^{1/2}$
Contracting volume (R_3)	$1-(1-\alpha)^{1/3}$	$2(1-\alpha)^{1/3}$
(3.2) Based on diffusion mechanisms		
One-dimentional (D_1)	$1/2\alpha^2$	α^{-1}
Two-dimensional (D_2)	$(1-\alpha)\ln(1-\alpha)+\alpha$	$[-\ln(1-\alpha)]^{-1}$
Three-dimensional (D_3)	$[1-(1-\alpha)^{1/3}]^2$	$2/3(1-\alpha)^{2/3}\,[1-(1-\alpha)^{1/3}]^{-1}$
Ginstling–Brounshtein (D_4)	$(1-2\alpha/3)-(1-\alpha)^{2/3}$	
(3.3) Based on "order" of reaction		
First-order (F_1)	$-\ln(1-\alpha)$	$(1-\alpha)$
Second-order (F_2)	$(1-\alpha)^{-1}$	$(1-\alpha)^2$
Third-order (F_3)	$(1-\alpha)^{-2}$	$1/2(1-\alpha)^3$

to determine the reaction mechanism. That is, plot $z(a)=f(a)\cdot g(a)$ against a for all possible mechanisms and thus establish a series of standard curves, the curve that best fits the experimental data in the form of

$$z(\alpha) = \frac{\mathrm{d}\alpha/\mathrm{d}t}{\beta} \cdot \pi(x) \cdot T, \tag{4}$$

where $\pi(x)=(x^3+18x^2+88x+96)/(x^4+20x^3+120x^2+240x+120)$, $x=E_a/RT$, and β represents the heating rate, should be considered as the reaction mechanism.

Afterwards, Achar, Brindley and Sharp equation [14], referred to as differential method

$$\ln\left(\frac{1}{f(\alpha)} \cdot \frac{\mathrm{d}\alpha}{\mathrm{d}T}\right) = \ln\left(\frac{A}{\beta}\right) - \frac{E_a}{RT}, \tag{5}$$

and Coats and Redfern equation [13], referred to as integral method

$$\log\left(\frac{g(\alpha)}{T^2}\right) = \log\left(\frac{AR}{E\beta}\right) - \frac{E_a}{RT}, \tag{6}$$

are further used to confirm the obtained activation energy.

Eq. (5) can be modified as

$$\ln\left(\frac{\mathrm{d}\alpha}{\mathrm{d}T}\beta\right) = \ln(Af(\alpha)) - \frac{E_a}{RT}, \tag{7}$$

for a certain α, $\ln(Af(\alpha))$ is constant. A plot of $\ln(\mathrm{d}\alpha/\mathrm{d}T\cdot\beta)$ against $1/T$ with varied β should allow the calculation of E_a. It shows that the activation energy changes slightly with α. The kinetic compensation law [15]

$$\ln A = bE + c, \tag{8}$$

is then introduced to correlate the pre-exponential factor A with E_a.

3. Experiments and results

3.1. Experiments

Purified CO_2 gas (about 20–40% concentration, diluted with N_2) bubbled though and carbonized 5–10% $Ca(OH)_2$ until the pH value reached 7–8. The precipitate was filtered, dried at 110°C to steady weight, then sifted through 320 mesh. The crystallite is confirmed as calcite by X-ray diffraction pattern and the particle size is estimated at around 40 nm by TEM

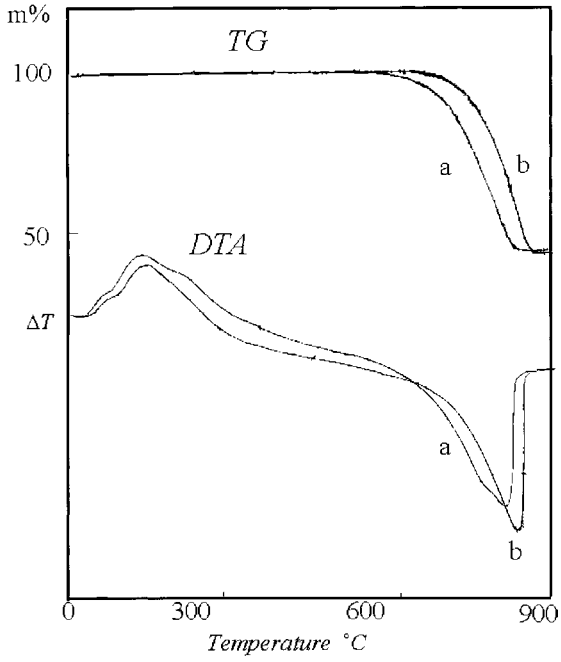

Fig. 1. Thermal curves of (a) nano-crystalline calcite and (b) reference calcite.

examining. A reference calcite (99.99%, the particle size is estimated at 5–20 μm by SEM examining) was used for comparison. All the experiments were performed on a shimadzu DT-30 thermal analyzer under

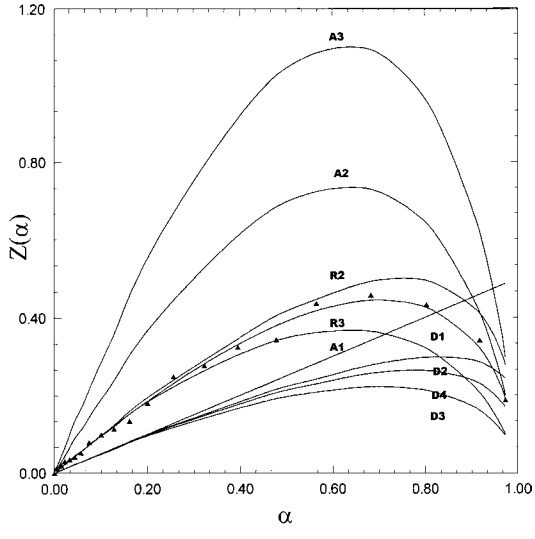

Fig. 2. Master curves of $z(\alpha)$ and experimental data (▲) for reference calcite at the heating rate of 20 K min^{-1}.

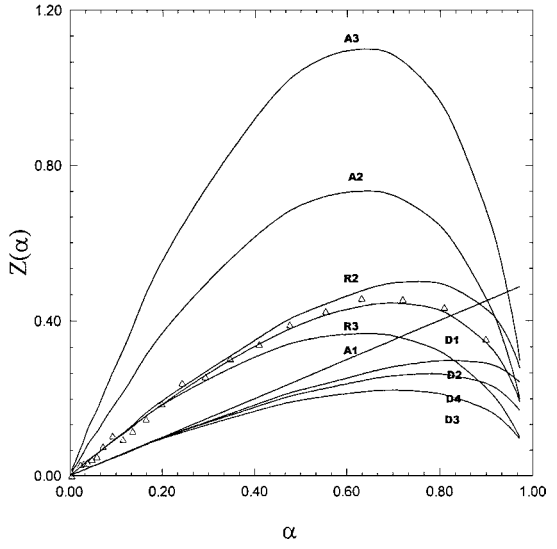

Fig. 3. Master curves of $z(\alpha)$ and experimental data (Δ) for nanocrystalline calcite at the heating rate of 20 K min^{-1}.

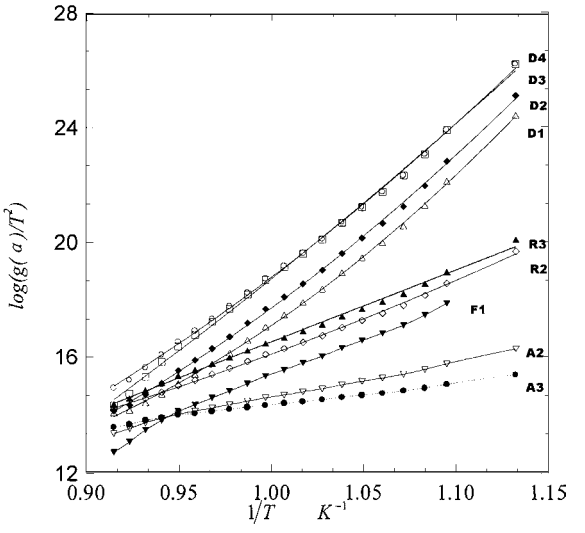

Fig. 4. $\log(g(a)/T^2)$ vs. $1/T$ for reference calcite: ($\bigcirc$) D_4; ($\square$) D_3; ($\blacklozenge$) D_2; (Δ) D_1; ($\blacktriangle$) R_3; ($\diamondsuit$) R_2; ($\blacktriangledown$) F_1; ($\triangledown$) A_2; ($\bullet$) A_3.

the protection of nitrogen gas flow. The heating rates for both reference and nanocrystalline calcites were at 5, 10, 20, and 50 K min^{-1}, respectively.

3.2. Decomposition mechanism and kinetic parameters

The thermal curves of reference and nanocrystalline calcite are shown as Fig. 1. There is a considerable left shift along the temperature axis in the case of nanocrystalline calcite. For each heating rate of the reference and nanocrystalline calcite, $\ln(T_p^2/\beta)$ is plotted against $1/T_p$ (Eq. (3)). Typical straight line fits the data points best. The corresponding activation energy E_a are 207.8 and 120.5 kJ mol^{-1}, respectively.

Utilizing the above obtained activation energy, $z(\alpha)$ for reference calcite and for nanocrystalline calcite at heating rate of 20 K min^{-1} are plotted against α as Figs. 2 and 3. It seems that R_3 (three-dimensional contracting volume model) fits the experimental data best in both cases.

For further confirmation of the reaction mechanism, using the experimental data of reference calcite and nanocrystalline calcite at heating rate of 20 K min^{-1},

Table 2
Determination of activation energy at different heating rates

Sample	Heating rate (K min^{-1})	E_a (kJ mol^{-1})	
		Differential method Achar, Brindley and Sharp	Integral method Coats and Redfern
Reference calcium carbonate	50	190.4	197.7
	20	196.2	201.7
	10	201.2	190.4
	5	199.5	187.1
Nano-particle calcium carbonate	50	125	117.7
	20	127.1	117.2
	10	130.4	121.4
	5	129.6	121.5

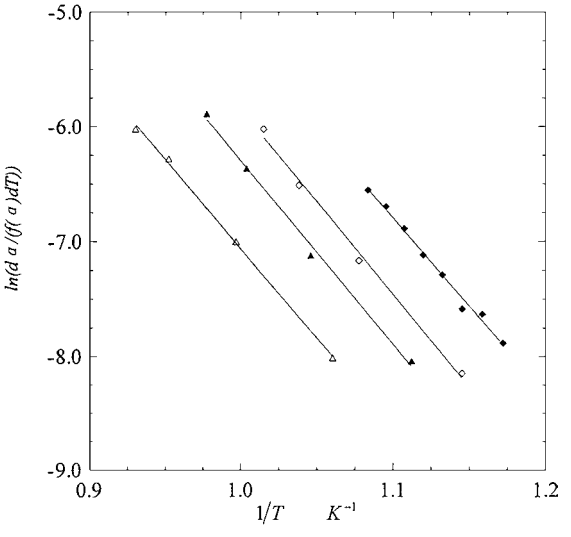

Fig. 5. $\ln(d\alpha/(f(\alpha)dT))$ vs. $1/T$ for nano-crystalline calcite: (Δ) 50 K min^{-1}; (▲) 20 K min^{-1}; (◇) 10 K min^{-1}; (◆) 5 K min^{-1}.

plot $\log(g(a)/T^2)$ against $1/T$ (as Eq. (6) shows). It is found that R_3 (contracting volume) mechanism curve is closer to straight line than other mechanisms. Fig. 4 shows the curves for the reference calcite case.

According to R_3 mechanism, for each heating rate of reference calcite and nanocrystalline calcite, differential method (Eq. (5)) and integral method (Eq. (6)) are used respectively to determine kinetic parameters. The corresponding values of E_a are listed in Table 2. Fig. 5 shows the curves for differential method in the case of nanocrystalline calcite.

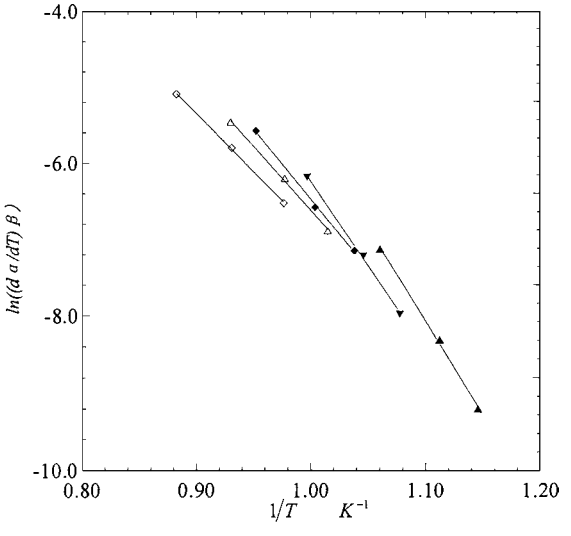

Fig. 6. $\ln((d\alpha/dT)\beta)$ vs. $1/T$ for nano-rystalline calcite at (◇) α=83.3%; (Δ) α=41.7%; (◆) α=27.8%; (▼) α=13.8%; (▲) α=5.56%.

It is shown that the activation energies of the tested samples increase slowly with the slowdown of the heating rate. It is also consistent with the estimated value obtained according to Eq. (3). Besides, the activation energy of nanocrystalline calcite has a diminution of up to 70–80 kJ mol^{-1} compared with reference calcite.

According to Eq. (7), a plot of $\ln((d\alpha/dT)\beta)$ against $1/T$ is shown as Fig. 6. Using different values of activation energy E_a and pre-exponential factor A obtained from Eq. (7), a correlation leads to the relationship of $\ln A = 0.1226 \cdot E - 7.468$ which fits literature value well [16].

4. Conclusions

1. Master plot method and Coats and Redfern equation substantiate that both nanocrystalline calcite and reference calcite dissociate according to contracting volume mechanism R_3, which is in accordance with most of the literature reports. Since the particle size is very small, D_1 and D_4 mechanisms reported in some literatures seem inappropriate in the case of nanocrystalline calcite.
2. The activation energy obtained from non-mechanism equation is consistent with that obtained from mechanism equation. It manifests the validity of both the reaction mechanism and the activation energy value. The activation energy of the reference calcite obtained from our experiments is approximately 200 kJ mol^{-1} and the value is in accordance with most of the reports.
3. The initial decomposition temperature of nanocrystalline calcite is much lower than reference calcite and there is a considerable diminution of activation energy up to 70–80 kJ mol^{-1} in the case of nanocrystalline calcite compared with the reference calcite. This diminution is usually attributed to the excessive energy stored on the surface of nano-material. However, through XRD experiments, it is recently found that the obvious aberrance and stress in the crystal lattice of nano-

material may contribute to its easier decomposition. The study about the influence of particle size using X-ray diffraction measurements is presently undergoing.

Acknowledgements

The authors thank Prof. Wu Qingzhou of the Analysis and Testing center of Zhejiang University for his help in the thermal analysis.

References

[1] C.D. Doyle, J. Appl. Polym. Sci. 5 (1961) 285.
[2] J. Zsako, J. Phys. Chem. 72 (1968) 2406.
[3] R.T. Rajeswara, Chem. Eng. Technol. 19 (1996) 373.
[4] J.M. Criado, J. Malek, A. Ortega, Thermochim. Acta 147 (1989) 377.
[5] J. Malek, Thermochim. Acta 200 (1992) 257.
[6] A.M. Gadalla, Thermochim. Acta 95 (1985) 179.
[7] A.M. Gadalla, Thermochim. Acta 74 (1984) 255.
[8] A.M. Mulokozi, E. Lugwisha, Thermochim. Acta 194 (1992) 375.
[9] J.M. Criado, A. Ortega, Thermochim. Acta 195 (1992) 163.
[10] E.S. Freeman, B. Carroll, J. Phys. Chem. 62 (1958) 394.
[11] H.E. Kissinger, J. Res. Notl. Bur. Stand 57 (1956) 712.
[12] V. Satava, Thermochim. Acta 2 (1971) 423.
[13] A.W. Coats, J.P. Redfern, Nature 201 (1964) 68.
[14] J.H. Sharp, S.A. Wendworth, Anal. Chem. 41 (1969) 2060.
[15] A.K. Galwey, Adv. Catal. 26 (1977) 247.
[16] D. Dollimors, Tong Ping, K. Alexander, Thermochim. Acta 282 283 (1996) 13.